

Quantum Computing for Atomic and Molecular Resonances

Teng Bian^{1,2,3} and Sabre Kais^{1,2,3,*}

¹*Department of Chemistry, Purdue University, West Lafayette, IN, 47907 USA*

²*Department of Physics and Astronomy, Purdue University, West Lafayette, IN, 47907 USA*

³*Purdue Quantum Science and Engineering Institute,
Purdue University, West Lafayette, IN, 47907 USA*

The complex-scaling method can be used to calculate molecular resonances within the Born-Oppenheimer approximation, assuming the electronic coordinates are dilated independently of the nuclear coordinates. With this method, one will calculate the complex energy of a non-Hermitian Hamiltonian, whose real part is associated with the resonance position and the imaginary part is the inverse of the lifetime. In this study, we propose techniques to simulate resonances on a quantum computer. First, we transformed the scaled molecular Hamiltonian to second-quantization and then used the Jordan-Wigner transformation to transform the scaled Hamiltonian to the qubit space. To obtain the complex eigenvalues, we introduce the Direct Measurement method, which is applied to obtain the resonances of a simple one-dimensional model potential that exhibits pre-dissociating resonances analogous to those found in diatomic molecules. Finally, we applied the method to simulate the resonances of the H_2^- molecule. Numerical results from the IBM Qiskit simulators and IBM quantum computers verify our techniques.

[Keywords]: Quantum computing, molecular systems, resonances, Direct Measurement method

I. INTRODUCTION

Resonances are intermediate or quasi-stationary states that exist during unique atomic processes such as: when an excited atom autoionizes, an excited molecule dissociates unimolecularly, or a molecule attracts an electron and then the ion disassociates into stable ionic and neutral subsystems[1]. The characteristics of resonances, such as energy and lifetime, can be revealed by experiments or predicted by theory. One theoretical method to compute properties associated with such resonances is called the complex-scaling method, developed by [2–7]. This method is based on the Balslev-Combes theorem, which is valid for dilation-analytic potentials and can be extended for non-dilation-analytic potential energies [8]. Additionally, several variants have been developed to study problems like Stark resonances[9–11] induced by an external electric field. The real space extension of this method uses standard quantum chemistry packages and stabilization graphs[12]. Its main applications are to study the decay of metastable states existing above the ionization threshold of Li centre in open-shell systems LiHe [13], in the computation of transition amplitudes among metastable states[14], and in explaining Autler-Townes splitting of spectral lines [15].

The complex-scaling method usually requires a large basis set to predict resonances with good accuracy. For example, the Helium 1S resonance uses 32 Hylleraas type functions for basis construction [16], and the H_2^- $^2\Sigma_u^+(\sigma_g^2\sigma_u)$ resonance takes a total of 38 constructed Gaussian atomic bases [8]. Computational overhead will become overwhelming if more basis functions need to be considered, like when simulating larger molecular systems, or requiring higher accuracy. Moreover, dimensional scaling and large-order dimensional perturbation theory have been applied for complex eigenvalues using the complex-scaling method [17, 18]. Like for bound states[19–23], quantum computing algorithms can overcome the above computational limitation problem for resonances. However, most algorithms cannot be directly adapted to resonance calculation with the complex-scaling method because the complex-rotated Hamiltonian is non-Hermitian. For example, the propagator $e^{-iH(re^{i\theta})t}$ in the conventional phase estimation algorithm (PEA) with trotterization [24] will be non-unitary and it cannot be implemented in a quantum circuit directly. In this way, a quantum algorithm for resonance calculation that can work with non-Hermitian Hamiltonians is needed. Daskin et al. [25] proposed a circuit design that can solve complex eigenvalues of a general non-unitary matrix. The method applies the matrix rows to an input state one by one and estimates complex eigenvalues via an iterative PEA process. However, for molecular Hamiltonians, the gate complexity of this general design is exponential in system size. In our previous publication[21], we briefly mentioned that our Direct Measurement method can solve complex eigenvalues of non-Hermitian Hamiltonians with polynomial gates. This study extends the Direct Measurement method and applies it to simple molecular systems as benchmark tests to obtain resonance properties. In particular, we will use IBM’s Qiskit [26] simulators and their quantum computers to calculate these resonances.

* kais@purdue.edu

In the following sections, we first show how to obtain the complex-scaled Hamiltonian for molecular systems and transform it into Pauli operator form. Then, we introduce the Direct Measurement method that can derive the Hamiltonian's complex eigenvalues. Finally, we apply this method to do resonance calculation for a simple model system and a benchmark test system H_2^- , using simulators and IBM quantum computers.

II. COMPLEX SCALED HAMILTONIAN

This section presents the steps needed to convert the complex-rotated Hamiltonian to a suitable form that can be simulated on a quantum computer. In the Born-Oppenheimer approximation, the electronic Hamiltonian of a molecular system can be written as a sum of electronic kinetic energy and potential energy of the form,

$$\begin{aligned} H(\mathbf{r}) &= T(\mathbf{r}) + V(\mathbf{r}), \\ T(\mathbf{r}) &= \sum_i -\frac{1}{2}\nabla_i^2, \\ V(\mathbf{r}) &= \sum_{i,j} \frac{1}{|\mathbf{r}_i - \mathbf{r}_j|} + \sum_{i,\sigma} \frac{Z_\sigma}{|\mathbf{r}_i - \mathbf{R}_\sigma|}, \end{aligned} \quad (1)$$

where Z_σ is the σ_{th} nucleus' charge, \mathbf{R}_σ is the σ_{th} nucleus' position, and $\mathbf{r}_i, \mathbf{r}_j$ represents the i_{th}, j_{th} electron's position. The complex scaling method is applied to the study of molecular resonances within the framework of Born-Oppenheimer approximation. Following Moiseyev et al.[27], the electronic coordinates are dilated independently of the nuclear coordinates. Given such a Hamiltonian $H(\mathbf{r})$ in Eq. (1), where \mathbf{r} represents electrons' coordinates, the complex-scaling method rotates \mathbf{r} into the complex plane by θ , $\mathbf{r} \rightarrow \mathbf{r}e^{i\theta}$. Thus the Hamiltonian becomes $H(\mathbf{r}e^{i\theta})$. After a complex rotation by θ , each electron's position \mathbf{r} becomes \mathbf{r}/η , where $\eta = e^{-i\theta}$ and thus the new Hamiltonian from Eq. (1) becomes

$$H_\theta = T(\mathbf{r}/\eta) + V(\mathbf{r}/\eta), \quad (2)$$

$$T(\mathbf{r}/\eta) = \eta^2 \sum_i -\frac{1}{2}\nabla_i^2, \quad (3)$$

$$V(\mathbf{r}/\eta) = \eta \sum_{i \neq j} \frac{1}{|\mathbf{r}_i - \mathbf{r}_j|} + \eta \sum_{i,\sigma} \frac{Z_\sigma}{|\mathbf{r}_i - \eta\mathbf{R}_\sigma|}. \quad (4)$$

It is shown that the system's resonance state's energy E and width $\Gamma = \frac{1}{\tau}$, where τ is the life time, are related to the corresponding complex eigenvalue of $H(\mathbf{r}e^{i\theta})$, [3, 28]

$$E_\theta = E - \frac{i}{2}\Gamma. \quad (5)$$

When doing exact calculation in an infinite basis limit, E_θ in Eq.(5) is not a function of θ . However, there would be dependence in reality because only a truncated basis set is always used in practice. The best resonance estimate is when the complex energy E_θ pauses or slows down in its trajectory [28, 29] in the (E_θ, θ) plane or $\frac{dE_\theta}{d\theta} = 0$. In this way, E and Γ can be obtained by solving the new Hamiltonian's eigenvalues for θ trajectories, and looking for the pause. A scaling parameter α is commonly used in the complex rotation process to locate better resonances, which makes $\eta = \alpha e^{-i\theta}$. We refer the readers to the book on non-Hermitian quantum mechanics by Moiseyev for more details and method applications [27].

After choosing a proper orthogonal basis set $\{\psi_i(\mathbf{r})\}$, the Hamiltonian can be converted into a second quantization form,

$$H_\theta = \sum_{i,j} h_{ij} a_i^\dagger a_j + \frac{1}{2} \sum_{i,j,k,l} h_{ijkl} a_i^\dagger a_j^\dagger a_k a_l, \quad (6)$$

In the equation, a_i^\dagger and a_i are fermionic creation and annihilation operators. The coefficients h_{ij}, h_{ijkl} can be

calculated by

$$\begin{aligned}
 h_{ij} &= \int \psi_i^*(\mathbf{r}) \left(-\eta^2 \frac{1}{2} \nabla_i^2 + \eta \sum_{\sigma} \frac{Z_{\sigma}}{|\mathbf{r} - \eta \mathbf{R}_{\sigma}|} \right) \psi_j(\mathbf{r}), \\
 h_{ijkl} &= \int \psi_i^*(\mathbf{r}_1) \psi_j^*(\mathbf{r}_2) \frac{\eta}{|\mathbf{r}_1 - \mathbf{r}_2|} \psi_k(\mathbf{r}_2) \psi_l(\mathbf{r}_1).
 \end{aligned}
 \tag{7}$$

With the Jordan-Wigner transformation[30],

$$\begin{aligned}
 a_j^{\dagger} &= \frac{1}{2} (X_j - iY_j) \otimes Z_{j-1}^{\rightarrow}, \\
 a_j &= \frac{1}{2} (X_j + iY_j) \otimes Z_{j-1}^{\rightarrow},
 \end{aligned}
 \tag{8}$$

in which X, Y and Z are the Pauli operators, and

$$Z_{j-1}^{\rightarrow} = Z_{j-1} \otimes Z_{j-2} \otimes Z_0,
 \tag{9}$$

the Hamiltonian in Eq.(6) will be further transformed into Pauli operators as

$$H_{\theta} = \sum_{i=0}^{L-1} c_i P_i.
 \tag{10}$$

In the summation, c_i represents a complex coefficient, and P_i represents a k -local tensor product of Pauli operators, where $k \leq n$ and n is the size of the basis set. Alternatively, the Bravyi-Kitaev transformation [30] or parity transformation can also be used in the final step for obtaining the Hamiltonian in the qubit space.

The above process is the same as the conventional Hamiltonian derivation in quantum computing for electronic structure calculations of bound states[19, 31–34]. Here for resonance calculations, to make the Hamiltonian more compatible with the Direct Measurement method, we rewrite Eq.(10) as

$$H_{\theta} = \sum_{i=0}^{2^{n_a}-1} \beta_i V_i,
 \tag{11}$$

where $n_a = \lceil \log_2 L \rceil$. The coefficient β_i and the operator V_i are determined in the following ways,

$$\begin{aligned}
 \beta_i &= |c_i|, V_i = \frac{c_i}{|c_i|} P_i, \quad \text{when } i < L, \\
 \beta_i &= 0, V_i = I, \quad \text{when } i \geq L.
 \end{aligned}
 \tag{12}$$

III. DIRECT MEASUREMENT METHOD

The Direct Measurement method is inspired by the direct application of the Phase Estimation Algorithm [35] as briefly discussed in our previous publication[21]. Here the basic idea is to apply the complex-rotated Hamiltonian to the state of the molecular system and obtain the complex energy information from the output state. Since the original non-Hermitian Hamiltonian cannot be directly implemented in a quantum circuit, this Direct Measurement method embeds it into a larger dimensional unitary operator.

Assuming n spin orbitals need to be considered for the system, the Direct Measurement method requires $n_s = n$ qubits to prepare the state of the model system $|\phi_r\rangle_s$ and an extra n_a ancilla qubits to enlarge the non-Hermitian Hamiltonian to be a unitary operator. The quantum circuit is shown in FIG. 1.

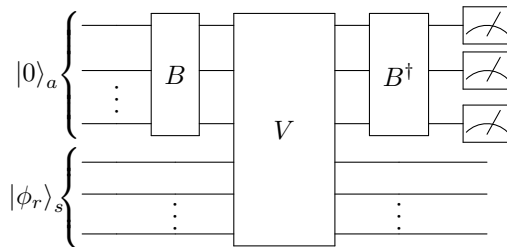


FIG. 1: The quantum circuit for Direct Measurement method. B and V gates are constructed based on the coefficients and operators in Eq.(11). The system qubits' state and ancilla qubits' state are initialized as $|0\rangle_a$ and $|\phi_r\rangle_s$ respectively.

The B and V gates in the circuit are designed to have the following properties

$$B|0\rangle_a = \sum_{i=0}^{2^{n_a}-1} \sqrt{\frac{\beta_i}{A}} |i\rangle_a, A = \sum_{i=0}^{2^{n_a}-1} \beta_i \quad (13)$$

$$V|i\rangle_a |\phi_r\rangle_s = |i\rangle_a V_i |\phi_r\rangle_s, \quad (14)$$

which means B transforms the initial ancilla qubits' state to a vector of coefficients, and V applies all V_i on system qubits based on ancilla qubits' states. One construction choice for B could be implementing the unitary operator

$$B = 2 \left(\sum_{i=0}^{2^{n_a}-1} \sqrt{\frac{\beta_i}{A}} |i\rangle_a \right) \left(\sum_{i=0}^{2^{n_a}-1} \sqrt{\frac{\beta_i}{A}} \langle i|_a \right) - I. \quad (15)$$

As for V , a series of multi-controlled V_i gates will do the work. If $|\phi_r\rangle_s$ is chosen as an eigenstate and we apply the whole circuit of B , V , and B^\dagger

$$U_r = (B^\dagger \otimes I^{\otimes n_s}) V (B \otimes I^{\otimes n_s}), \quad (16)$$

on it, the output state will be

$$U_r |0\rangle_a |\phi\rangle_s = \frac{E e^{i\varphi}}{A} |0\rangle_a |\phi\rangle_s + |\Phi^\perp\rangle, \quad (17)$$

where $E e^{i\varphi}$ ($E \geq 0$) is the corresponding eigenvalue and $|\Phi^\perp\rangle$ is a state whose ancilla qubits' state is perpendicular to $|0\rangle_a$. Then we can derive E by measuring the output state. To obtain the phase φ , we apply a similar circuit for $H'_\theta = x I^{\otimes n} + H_\theta$, where x is a selected real number, and perform the measurements. The calculation details are found in Appendix C.

IV. QUANTUM SIMULATION OF RESONANCES IN A SIMPLE MODEL SYSTEM

In this section, we calculate the resonance properties of a model system using the Direct Measurement method. This system is the following one-dimensional potential[28]

$$V(x) = \left(\frac{1}{2}x^2 - J\right)e^{-\lambda x^2} + J, \quad (18)$$

and parameters are chosen as $\lambda = 0.1$, $J = 0.8$. The potential plot is in FIG. 2. This potential is used to model some resonance phenomena in diatomic molecules. We only consider one electron under this potential. The original

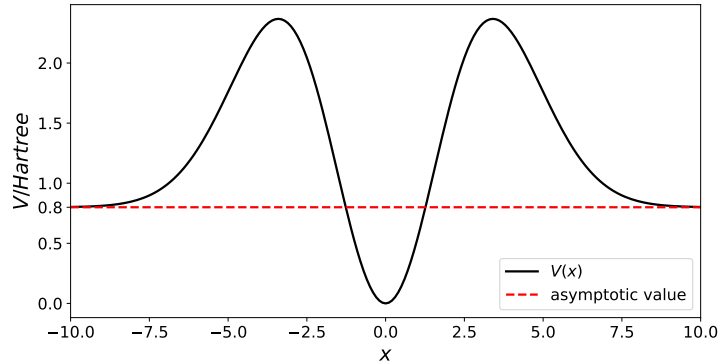


FIG. 2: The one-dimensional potential $V(x) = (\frac{1}{2}x^2 - J)e^{-\lambda x^2} + J$, where $\lambda = 0.1$, $J = 0.8$.

Hamiltonian and the complex-rotated Hamiltonian can be written as

$$H = -\frac{\nabla_x^2}{2} + V(x), \quad (19)$$

$$H_\theta = -\eta^2 \frac{\nabla_x^2}{2} + V(\eta x) \quad (20)$$

To make the setting consistent with the original literature, η is chosen to be $e^{-i\theta}$ and the scaling parameter α is embedded in n Gaussian basis functions

$$\chi_k(\alpha) = \exp(-\alpha_k x^2), \quad (21)$$

$$\alpha_k = \alpha(0.45)^k, k = 0, 1, \dots, n-1. \quad (22)$$

The $\{\chi_k(\alpha)\}$ basis set is not orthogonal, so we apply Gram-Schmidt process and iteratively construct an orthogonal basis set $\{\psi_i\}$ as follows:

$$\gamma_k = \chi_k - \sum_{i=0}^{k-1} \langle \chi_k | \psi_i \rangle \psi_i, \quad (23)$$

$$\psi_i = \frac{\gamma_k}{\|\gamma_k\|} = \frac{\gamma_k}{\sqrt{\langle \gamma_k | \gamma_k \rangle}}. \quad (24)$$

Since there is only one electron, we do not consider spin interactions. This $\{\psi_i\}$ basis set is used in the second quantization step to get the final Hamiltonian in Pauli matrix form. The resonance eigenvalue found in [28] with $n = 10$ basis functions is $E_\theta = 2.124 - 0.019i$ Hartree. We will try to get the same resonance by applying the Direct Measurement method using the Qiskit package. The Qiskit package supports different backends, including a statevector simulator that executes ideal circuits, a QASM simulator that provides noisy gate simulation, and various quantum computers. In the following section, we show the results when the basis function number is $n = 5$ and $n = 2$. In particular, the former $n = 5$ case shows how θ trajectories locate the best resonance estimate, and the latter $n = 2$ cases show how to further simplify the quantum circuit for the Direct Measurement method and run it on IBM quantum computers.

C1 in the Table I is our primary example where we follow the above steps in section II and III for $n = 5$. An example of the complex-rotated Hamiltonian is shown in Appendix A. FIG. 3 shows a sweep of scaling parameters α , for statevector simulations of θ trajectories. Most trajectories pause around the point, $E_\theta = 2.1265 - 0.0203i$ Hartree, when $\alpha = 0.65$, $\theta = 0.160$. Based on Eq.(5), this indicates the resonance energy and width are $E = 2.1265$ Hartree, $\Gamma = 0.0406$ Hartree, close to the resonance energy from [28]. The IBM quantum computer cannot perform the method due to a large number of standard gates in the circuit. Instead, we used the QASM simulator for $4 * 10^4$ shots and obtained the system's resonance energy at $\alpha = 0.65$, $\theta = 0.160$, $E_\theta = 2.1005 - 0.3862i$ Hartree. This result has an error of around 0.3 Hartree but can be augmented by more sample measurements.

Case Name	#Basis functions	#Total Qubits	#System Qubits	#Ancilla Qubits	#Gates
C1	5	10	5	5	$\sim 10^6$
C2	2	5	2	3	~ 800
C3	2	4	2	2	~ 200
C4	2	3	2	1	~ 10

TABLE I: The number of qubits and estimated gates in different cases when the Direct Measurement method is used to calculate resonance properties for the model system. The estimation for gate numbers is based on the QASM simulator and IBM machines.

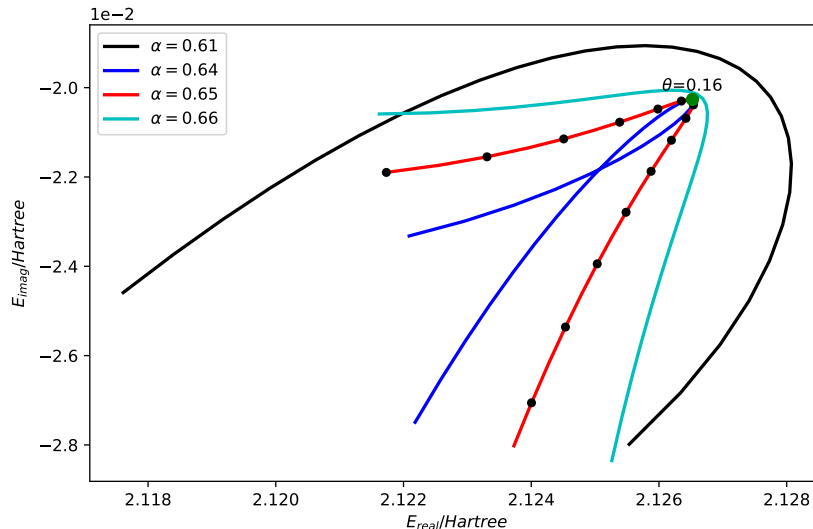


FIG. 3: Trajectories of a complex eigenvalue on the rotation angle θ for fixed $n = 5$ and various α , calculated by Qiskit statevector simulator. θ ranges from 0.1 to 0.24 with a step of 0.01. The green point shows the best estimation of resonance energy, which is $E = 2.1265 - 0.0203i$ Hartree, occurs at $\alpha = 0.65, \theta = 0.160$. The input state for the Direct Measurement method is obtained by directly diagonalizing the complex-rotated Hamiltonian matrix.

When taking $n = 2$ for the basis function, we are not able to locate the best resonance estimate, see FIG. 3, based on direct diagonalization. So, we only use the Direct Measurement method to calculate the complex eigenenergy when $\alpha = 0.65$ and $\theta = 0.160$, where the best location is at $n = 5$. We run the Direct Measurement method using simulators first and then try to reduce the number of ancilla qubits to make the resulting circuit short enough to be executed in the IBM quantum computers.

C2 in TABLE I is the case when we follow the steps for $n = 2$ in section II and III. The Hamiltonian H_θ and how to calculate its complex eigenvalue are shown in Appendix D.A Eq.(30). FIG. 4 gives the quantum circuit for H_θ . This circuit can be executed in simulators with results listed in TABLE II.

Method	Eigenenergy (Hartree)	Error (Hartree)
Direct Diagonalization	2.1259-0.1089i	-
Statevector Simulator	2.1259-0.1089i	0
QASM Simulator	2.1279-0.1100i	2×10^{-3}

TABLE II: The complex eigenenergy obtained by directly diagonalizing the Hamiltonian and by running different simulators. The QASM simulator is configured to have no noise, and it takes 10^5 samples to calculate the complex eigenenergy.

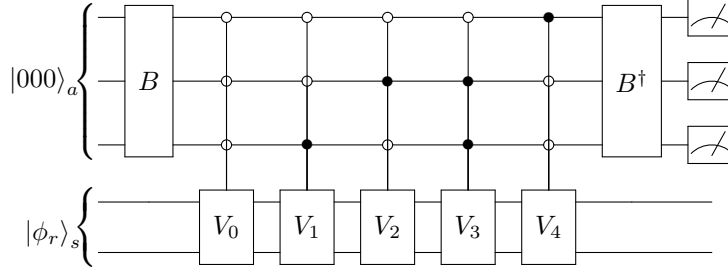


FIG. 4: The quantum circuit to run Direct Measurement method when $n = 2$. B gate is prepared by the coefficients $[1.31556, 0.13333, 0.13333, 0.25212, 1.06378]$. V_0, V_1, V_2, V_3 and V_4 are applying $e^{-0.04180i}II$ and $e^{2.32888i}YY, e^{2.32888i}XX, e^{3.05283i}ZI$ and $e^{3.11093i}IZ$ respectively.

However, it is too complicated to be successfully run in IBM quantum computers. For C3 in TABLE I, we simplify the quantum circuit by calculating the complex eigenvalue for the Hamiltonian H_θ in Appendix D.B, Eq. (32). Because there are only 4 terms left, 2 ancilla qubits are enough for the method. The simplified quantum circuit is then shown in FIG. 5. To avoid introducing more ancilla qubits, instead of $H'_\theta = H_\theta + xII$, we can run a similar

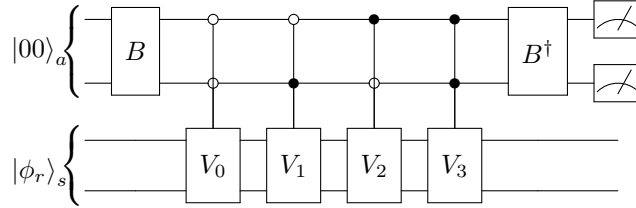


FIG. 5: The simplified quantum circuit to run Direct Measurement method when $n = 2$. B gate is prepared by the coefficients $[0.13333, 0.13333, 0.25212, 1.06378]$. V_0, V_1, V_2 and V_3 are applying $e^{2.32888i}YY, e^{2.32888i}XX, e^{3.05283i}ZI$ and $e^{3.11093i}IZ$ respectively.

4-qubit circuit for $H'_\theta = H_\theta + H_\theta^3$, which has the same terms of tensor products as H_θ with different coefficients. This

Method	Eigenenergy (Hartree)	Error (Hartree)
Direct Diagonalization	2.1259-0.1089i	-
Statevector Simulator	2.1259-0.1089i	0
QASM Simulator	2.1264-0.1099i	1×10^{-3}
IBM Quantum Computer	2.0700-0.4890i	0.3841

TABLE III: The complex eigenenergy obtained by directly diagonalizing the Hamiltonian, running simulators and using IBM quantum computers. The QASM simulator is configured to be noiseless, and it takes 10^5 samples to calculate the complex eigenenergy. The IBM quantum computer takes 2^{13} samples.

circuit can be executed successfully in the simulators and the IBM quantum computers. However, it costs around 200 gates in the IBM quantum computers, leading to significant error. The resulting resonance eigenenergies and errors can be seen in TABLE. III.

For the Hamiltonian Eq.(32), a simpler circuit can be constructed if we try to calculate the complex eigenvalue of its square, Eq.(35) in Appendix D.C. This is C4 in TABLE. I. The quantum circuit for this H_θ^2 is showed in FIG. 6.

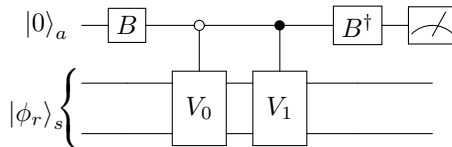


FIG. 6: The quantum circuit to run Direct Measurement method when $n = 2$. B gate is prepared by the coefficients [1.19577, 0.53529]. V_0, V_1 are applying $e^{-0.09723i}II$ and $e^{-0.05311i}ZZ$ respectively.

We can also run a similar 3-qubit circuit for $(H_\theta^2)' = H_\theta^2 + H_\theta^4$. The implementation of the circuit costs 9 gates in the IBM quantum computers after circuit optimization. The resulting eigenenergies are in TABLE. IV.

Method	Eigenenergy (Hartree)	Error (Hartree)
Direct Diagonalization	2.1259-0.1089i	-
Statevector Simulator	2.1259-0.1089i	0
QASM Simulator	2.1259-0.1107i	1.7×10^{-3}
IBM Quantum Computer	2.1624-0.1188i	0.0378

TABLE IV: The complex eigenenergy obtained by directly diagonalizing the Hamiltonian, running simulators and running IBM quantum computers. The QASM simulator is configured to be noiseless, and it takes 10^5 samples to calculate the complex eigenenergy. The IBM quantum computer takes 2^{13} samples. The error of the IBM quantum computer is from the best case.

V. QUANTUM SIMULATION OF THE RESONANCES IN H_2^-

This section presents a proof of concept that by using our quantum algorithm, the Direct Measurement method, one can calculate molecular resonances on a quantum computer. We focus on the resonances of a simple diatomic molecule, H_2^- $^2\Sigma_u^+(\sigma_g^2\sigma_u)$. Moiseyev and Corcoran [8] showed how to obtain this molecule's resonance using a variational method based on the (5s,3p,1d/3s,2p,1d) contracted Gaussian atomic basis, which contains a total of 76 atomic orbitals for H_2^- . They picked around 45 configurations of natural orbitals as a final basis for resonance calculation. Here, however, we are not going to use their contracted Gaussian atomic basis, that needs 76 system qubits with additional ancilla qubits, which is too large to be simulated by classical computers. The number of gates would also be overwhelming. One may try an iterative diagonalization approach to get a few eigenvalues without constructing matrices or vectors. Another possible solution could be using tensor network simulators. Recent studies by Ellerbrock and Martinez show that tensor network simulators are able to efficiently and accurately simulate over 100-qubit circuits with moderate entanglement [36]. In another study Zhou et al. showed that even strongly entangled systems (as those generated by 2D random circuits) can be simulated by matrix product states comparably accurate to modern quantum devices [37]. However, building those simulators for our system is beyond the scope of this paper. In this way, we picked small basis sets, 6-31g, and cc-pVDZ, for our simulations. We used the Born-Oppenheimer approximation followed by complex rotation, as shown in Section II, "COMPLEX SCALED HAMILTONIAN" and mapped the Hamiltonian to the qubit space, as shown in Appendix B. We then apply the Direct Measurement method to the Hamiltonian to obtain complex eigenvalues. An example quantum circuit to run the Direct Measurement method can be found in Appendix E.

FIG. 7 shows one complex eigenvalue's θ trajectories at $\alpha = 1.00$ under different basis sets after running the algorithm. FIG. 7.(a) is simulated using the 6-31g basis set. 8 spin-orbitals are considered in our self-defined simulator, and 16 qubits are needed to run the algorithm. In this case, if we fix $\eta = \alpha e^{-i\theta}$ at the lowest point in the figure, which has $\alpha = 1.00$, $\theta = 0.18$, the resonance energy obtained by the Direct Measurement method is $E_\theta = -0.995102 - 0.046236i$ Hartree. This complex energy is close to the one obtained in [8], $E_\theta = -1.0995 - 0.0432i$ Hartree, especially the imaginary part. FIG. 7.(b) is simulated using the cc-pVDZ basis set. We only considered the s and p_z basis functions for H atom for easier simulation. 12 spin-orbitals are considered in our self-defined simulator, and a total of 23 qubits are needed to run the algorithm in quantum computers. The results show the resonance energy at the lowest point in the figure, which has $\alpha = 1.00$, $\theta = 0.22$, is $E_\theta = -1.045083 - 0.044513i$ Hartree. This is even closer to the one obtained in [8]. However, we want to note that the lowest points in FIG. 7 (a) and FIG. 7 (b) are not pause points. And they do not reveal real resonance properties. Also, even after shifting different α in simulations,

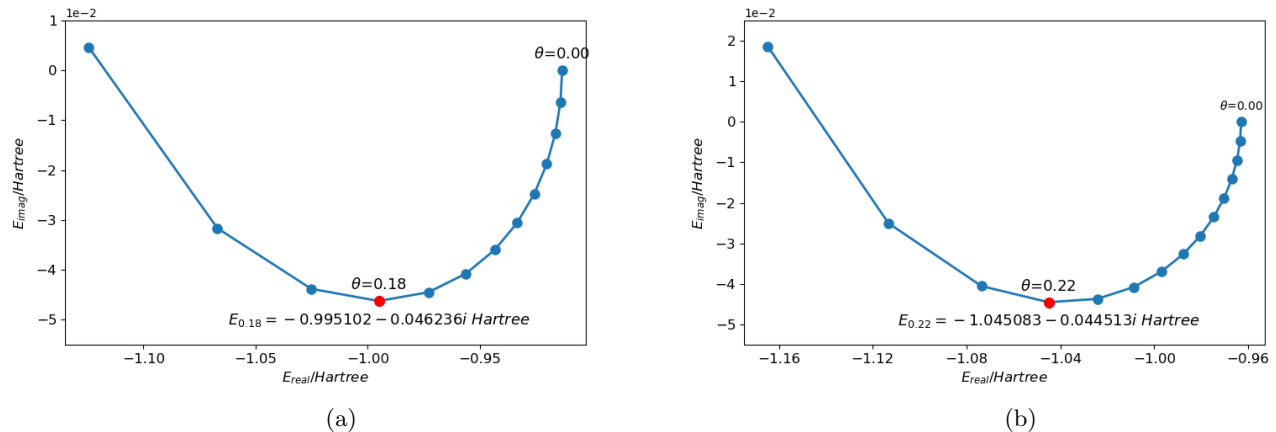


FIG. 7: Complex eigenvalue trajectories on the rotation angle θ at $\alpha = 1.00$ for molecule H_2^- , calculated by a self-defined simulator. (a) uses 6-31g basis set for H atom, including 1s and 2s orbitals. θ ranges from 0.00 to 0.24 with a step of 0.02. At the lowest point when $\theta = 0.18$, the complex eigenvalue is $-0.995102 - 0.046236i$ Hartree. (b) uses the s and p_z orbitals in cc-pVDZ basis set for H atom. θ ranges from 0.00 to 0.28 with a step of 0.02. At the lowest point when $\theta = 0.22$, the complex eigenvalue is $-1.045083 - 0.044513i$ Hartree.

we cannot find a consistent pause point in θ trajectories to locate the best resonance estimation. The reason may be related to our selected basis. Compared with the literature [8], our basis set is much smaller, and is not optimized for the resonance state. Still, this application gives proof of concept and shows that one can calculate molecular resonances on a quantum computer. In the future, if more qubits are available in quantum computers, a large basis can be used, and we may be able to show finer structures in trajectories that can locate the best resonance point. Also, a larger basis set should lead to a more accurate resonance calculation.

VI. CONCLUSION

In this paper, we construct and show a proof-of-concept for a quantum algorithm that calculates atomic and molecular resonances. We first presented the complex-scaling method to calculate molecular resonances. Then, we introduced the Direct Measurement method, which embeds a molecular system's complex-rotated Hamiltonian into the quantum circuit and calculates the resonance energy and lifetime from the measurement results. These results represent the first applications of complex scaling Hamiltonian to molecular resonances on a quantum computer. The method is proven to be accurate when applied to a simple one-dimensional quantum system that exhibits shape resonances. We tested our algorithm on quantum simulators and IBM quantum computers. Furthermore, when compared to the exponential time complexity in traditional matrix-vector multiplication calculations, this method only requires $O(n^5)$ standard gates, where n is the size of the basis set. These findings show this method's potential to be used in a more complicated molecular system and for better accuracy in the future when more and better qubit machines are available.

VII. ACKNOWLEDGEMENTS

We would like to thank Rongxin Xia, Zixuan Hu, and Manas Sajjan for useful discussions. We also like to acknowledge the financial support by the National Science Foundation under award number 1955907.

VIII. DATA AVAILABILITY

The data that support the findings of this study are available from the corresponding author upon reasonable request.

-
- [1] William P Reinhardt, “Complex coordinates in the theory of atomic and molecular structure and dynamics,” *Annual Review of Physical Chemistry* **33**, 223–255 (1982).
 - [2] Jacques Aguilar and Jean-Michel Combes, “A class of analytic perturbations for one-body schrödinger hamiltonians,” *Communications in Mathematical Physics* **22**, 269–279 (1971).
 - [3] Erik Balslev and Jean-Michel Combes, “Spectral properties of many-body schrödinger operators with dilatation-analytic interactions,” *Communications in Mathematical Physics* **22**, 280–294 (1971).
 - [4] Barry Simon, “Quadratic form techniques and the balslev-combes theorem,” *Communications in Mathematical Physics* **27**, 1–9 (1972).
 - [5] Barry Simon, “Resonances in n-body quantum systems with dilatation analytic potentials and the foundations of time-dependent perturbation theory,” *Annals of Mathematics* , 247–274 (1973).
 - [6] Clasine van Winter, “Complex dynamical variables for multiparticle systems with analytic interactions. i,” *Journal of Mathematical Analysis and Applications* **47**, 633–670 (1974).
 - [7] Nimrod Moiseyev, “Quantum theory of resonances: calculating energies, widths and cross-sections by complex scaling,” *Physics reports* **302**, 212–293 (1998).
 - [8] Nimrod Moiseyev and Chris Corcoran, “Autoionizing states of h 2 and h 2- using the complex-scaling method,” *Physical Review A* **20**, 814 (1979).
 - [9] Agapi Emmanouilidou and Linda E Reichl, “Scattering properties of an open quantum system,” *Physical Review A* **62**, 022709 (2000).
 - [10] Yuki Orimo, Takeshi Sato, Armin Scrinzi, and Kenichi L Ishikawa, “Implementation of the infinite-range exterior complex scaling to the time-dependent complete-active-space self-consistent-field method,” *Physical Review A* **97**, 023423 (2018).
 - [11] Thomas-C Jagau, “Coupled-cluster treatment of molecular strong-field ionization,” *The Journal of chemical physics* **148**, 204102 (2018).
 - [12] Idan Haritan and Nimrod Moiseyev, “On the calculation of resonances by analytic continuation of eigenvalues from the stabilization graph,” *The Journal of chemical physics* **147**, 014101 (2017).
 - [13] Arie Landau, Anael Ben-Asher, Kirill Gokhberg, Lorenz S Cederbaum, and Nimrod Moiseyev, “Ab initio complex potential energy curves of the he*(1 s 2 p 1p)–li dimer,” *The Journal of chemical physics* **152**, 184303 (2020).
 - [14] Debarati Bhattacharya, Arie Landau, and Nimrod Moiseyev, “Ab initio complex transition dipoles between autoionizing resonance states from real stabilization graphs,” *The Journal of Physical Chemistry Letters* **11**, 5601–5609 (2020).
 - [15] Adi Pick, Petra Ruth Kaprálová-Žďánská, and Nimrod Moiseyev, “Ab-initio theory of photoionization via resonances,” *The Journal of chemical physics* **150**, 204111 (2019).
 - [16] N Moiseyev, PRr Certain, and F Weinhold, “Complex-coordinate studies of helium autoionizing resonances,” *International Journal of Quantum Chemistry* **14**, 727–736 (1978).
 - [17] S Kais and DR Herschbach, “Dimensional scaling for quasistationary states,” *The Journal of chemical physics* **98**, 3990–3998 (1993).
 - [18] Timothy C Germann and Sabre Kais, “Large order dimensional perturbation theory for complex energy eigenvalues,” *The Journal of chemical physics* **99**, 7739–7747 (1993).
 - [19] S. Kais, *Quantum Information and Computation for Chemistry: Advances in Chemical Physics*, Vol. 154 (Wiley Online Library, NJ, US., 2014) p. 224109.
 - [20] Rongxin Xia and Sabre Kais, “Quantum machine learning for electronic structure calculations,” *Nature communications* **9**, 1–6 (2018).
 - [21] Teng Bian, Daniel Murphy, Rongxin Xia, Ammar Daskin, and Sabre Kais, “Quantum computing methods for electronic states of the water molecule,” *Molecular Physics* **117**, 2069–2082 (2019).
 - [22] Ammar Daskin, Teng Bian, Rongxin Xia, and Sabre Kais, “Context-aware quantum simulation of a matrix stored in quantum memory,” *Quantum Information Processing* **18**, 357 (2019).
 - [23] Rongxin Xia, Teng Bian, and Sabre Kais, “Electronic structure calculations and the ising hamiltonian,” *The Journal of Physical Chemistry B* **122**, 3384–3395 (2017).
 - [24] Seth Lloyd, “Universal quantum simulators,” *Science* , 1073–1078 (1996).
 - [25] Amner Daskin, Ananth Grama, and Sabre Kais, “A universal quantum circuit scheme for finding complex eigenvalues,” *Quantum information processing* **13**, 333–353 (2014).
 - [26] Héctor Abraham et. al, “Qiskit: An open-source framework for quantum computing,” (2019).
 - [27] Nimrod Moiseyev, *Non-Hermitian quantum mechanics* (Cambridge University Press, 2011).
 - [28] N Moiseyev, PR Certain, and F Weinhold, “Resonance properties of complex-rotated hamiltonians,” *Molecular Physics* **36**, 1613–1630 (1978).
 - [29] GD Doolen, “A procedure for calculating resonance eigenvalues,” *Journal of Physics B: Atomic and Molecular Physics* **8**, 525 (1975).

- [30] Jacob T Seeley, Martin J Richard, and Peter J Love, “The bravyi-kitaev transformation for quantum computation of electronic structure,” *The Journal of chemical physics* **137**, 224109 (2012).
- [31] Peter JJ O’Malley, Ryan Babbush, Ian D Kivlichan, Jonathan Romero, Jarrod R McClean, Rami Barends, Julian Kelly, Pedram Roushan, Andrew Tranter, Nan Ding, *et al.*, “Scalable quantum simulation of molecular energies,” *Physical Review X* **6**, 031007 (2016).
- [32] Alán Aspuru-Guzik, Anthony D Dutoi, Peter J Love, and Martin Head-Gordon, “Simulated quantum computation of molecular energies,” *Science* **309**, 1704–1707 (2005).
- [33] Yudong Cao, Jonathan Romero, Jonathan P Olson, Matthias Degroote, Peter D Johnson, Mária Kieferová, Ian D Kivlichan, Tim Menke, Borja Peropadre, Nicolas PD Sawaya, *et al.*, “Quantum chemistry in the age of quantum computing,” *Chemical reviews* **119**, 10856–10915 (2019).
- [34] Jarrod McClean, Nicholas Rubin, Kevin Sung, Ian David Kivlichan, Xavier Bonet-Monroig, Yudong Cao, Chengyu Dai, Eric Schuyler Fried, Craig Gidney, Brendan Gimby, *et al.*, “Openfermion: the electronic structure package for quantum computers,” *Quantum Science and Technology* (2020).
- [35] Ammar Daskin and Sabre Kais, “Direct application of the phase estimation algorithm to find the eigenvalues of the hamiltonians,” *Chemical Physics* **514**, 87–94 (2018).
- [36] Roman Ellerbrock and Todd J Martinez, “A multilayer multi-configurational approach to efficiently simulate large-scale circuit-based quantum computers on classical machines,” *The Journal of Chemical Physics* **153**, 051101 (2020).
- [37] Yiqing Zhou, E Miles Stoudenmire, and Xavier Waintal, “What limits the simulation of quantum computers?” *Physical Review X* **10**, 041038 (2020).

APPENDIX A

COMPLEX-ROTATED HAMILTONIAN OF THE MODEL SYSTEM AT $\theta = 0.16$, $\alpha = 0.65$ WHEN $n = 5$

YYIII	-0.091665+0.096819i	XXIII	-0.091665+0.096819i	IIIII	4.599205-0.533073i
ZIII	-0.251131+0.022353i	YZYII	0.0179156-0.030997i	XZXII	0.0179156-0.030997i
YZZYI	-0.007005+0.015446i	XZZXI	-0.007005+0.015446i	YZZZY	0.003680-0.009152i
XZZZX	0.003680-0.009152i	IZIII	-1.063280+0.032614i	IYYII	-0.089297+0.108259i
IXXII	-0.089297+0.108259i	IYZYI	0.014213-0.055870i	IXZXI	0.014213-0.055870i
IYZZY	-0.003869+0.033693i	IXZZX	-0.003869+0.033693i	IIZII	-1.445349+0.113618i
IYYI	-0.209952+0.010748i	IIXXI	-0.209952+0.010748i	IYZY	0.060302-0.008776j
IIXZX	0.060302-0.008776i	IIIZI	-1.127058+0.243702i	IIYY	-0.336956+0.051691i
IIIX	-0.336956+0.051691i	IIIZ	-0.712385+0.120784i		

TABLE V: The coefficients and tensor product operators of the model system's complex-rotated Hamiltonian H_θ at $\theta = 0.16$, $\alpha = 0.65$ when there is $n = 5$ basis functions.

APPENDIX B

COMPLEX-ROTATED HAMILTONIAN OF H_2^- AT $\theta = 0.18$, $\alpha = 1.00$

IXZXXZXI	0.018705 -0.003404i	IIIZIXZX	0.038191 -0.006950i	ZIZIIII	0.103932 -0.018913i
XZXIXZXI	0.027826 -0.005063i	IXXIIIXX	-0.002794+0.000508i	IIZZIIII	0.106657 -0.019408i
IYIYIIII	0.024307 -0.004423i	IIIIXXXX	0.015119 -0.002751i	IZIIIIZI	0.095226 -0.017328i
IIIIIXX	0.047512 -0.039979i	YYIIYZZY	-0.019254+0.003504i	XZXIYZYI	0.027826 -0.005063i
IZIIZZYI	0.013080 -0.002380i	IYYIIXX	0.034554 -0.006288i	XZXIIIZI	0.032587 -0.005930i
YYYYIIII	0.015119 -0.002751i	XXIIYYI	0.005216 -0.000949i	IXIXIIII	0.024307 -0.004423i
IIIXXXY	0.002918 -0.000531i	IIIZXZXI	0.050249 -0.009144i	IIXXXXII	0.020481 -0.003727i
YYIIYYII	0.019597 -0.003566i	IXXIIXXI	0.008283 -0.001507i	IIIXIXI	0.016733 -0.003045i
IYZYIIII	-0.035671+0.030324i	IYZYIIIZ	0.043018 -0.007828i	YYIIYYI	0.005216 -0.000949i
IIIXZZX	-0.028316+0.033738i	XXIIYYII	0.019597 -0.003566i	IXXIIYY	-0.002794+0.000508i
ZYZYIIII	0.015436 -0.002809i	XXIIYZZY	-0.019254+0.003504i	IIIIZZI	0.084620 -0.015398i
YZYIIZII	0.011702 -0.002129i	IYYXZZX	-0.031698+0.005768i	IIIIXXI	-0.007550+0.006494i
IXXIZIZI	0.012371 -0.002251i	IIIIYYYY	0.015119 -0.002751i	IIIZYZYI	0.050249 -0.009144i
ZIIIIII	-0.230405+0.108639i	ZIIIIIZ	0.159054 -0.028943i	IXXIYZZY	0.006593 -0.001200i
IIIIYIY	0.023153 -0.004213i	IYYIXXI	-0.000541+0.000098i	YZZYIIII	-0.027204+0.031862i
IIIZIIZI	0.139579 -0.025399i	YZZYXXII	-0.016647+0.003029i	IIXXIIII	0.047746 -0.040370i
XIXIIII	0.017118 -0.003115i	YYIIXXII	0.019597 -0.003566i	YZYIYZY	0.017127 -0.003117i
IIIIZZII	0.084496 -0.015376i	YZZYXZZX	0.031161 -0.005670i	IIIZIYZY	0.024717 -0.004498i
XZZXIXXI	0.004990 -0.000908i	IYYIIYYI	0.008283 -0.001507i	IYZYIXZX	0.015728 -0.002862i
XZZXXZZX	0.031161 -0.005670i	IYZYIIZI	0.026040 -0.004739i	IIIZIIZI	0.093507 -0.017015i
IZIIZIII	0.106161 -0.019318i	XXIIIXXI	0.005216 -0.000949i	IXZXIYZY	0.015728 -0.002862i
ZIIIXZX	0.030922 -0.005627i	IIIIYY	0.047512 -0.039979i	XXIIYY	0.021209 -0.003859i
XXIIIXX	0.021209 -0.003859i	YYIIII	0.001646 -0.022572i	ZIIIIZI	0.130169 -0.023687i
IYYIYY	0.034554 -0.006288i	YZYIIIZ	0.052229 -0.009504i	YZYIIII	-0.021561+0.077956i
IIXXXZZX	-0.031698+0.005768i	IIIZYZY	0.013729 -0.002498i	IYYIXXII	0.003919 -0.000713i
IIIZIIZI	0.133407 -0.024276i	YZZYZZY	0.031161 -0.005670i	XZXIZIIZ	0.040337 -0.007340i
ZIIIZIIZ	0.151365 -0.027544i	YZYIIXZX	0.017127 -0.003117i	IIIIYIY	0.016733 -0.003045i
IIXXIYYI	-0.000541+0.000098i	IYYYYZZY	-0.031698+0.005768i	IYYIIII	-0.009705+0.008779i
YZZYYYII	-0.016647+0.003029i	XZXIIXZX	0.017127 -0.003117i	IIIIIXIX	0.023153 -0.004213i
IIIZIYZYI	0.033580 -0.006110i	ZXZXIIII	0.015436 -0.002809i	YZYZIIII	0.020644 -0.003757i
IIIIYZZY	-0.028316+0.033738i	IXXZIIII	0.034152 -0.006215i	YZZYIYYI	0.004990 -0.000908i
ZIIZIIZI	0.126456 -0.023011i	YZZYIIXX	-0.029557+0.005379i	XZZXYZZY	0.031161 -0.005670i
IYYIYY	-0.002794+0.000508i	IXXIIII	-0.035671+0.030324i	IXXIIIZ	0.043018 -0.007828i
ZIIZYZYI	0.038659 -0.007035i	IIXXIIXX	0.034554 -0.006288i	ZZIIII	0.085046 -0.015476i
IIIZIIZI	0.158431 -0.028830i	YXXYIIII	0.012162 -0.002213i	IZIIZYZY	0.013159 -0.002395i
IYZYXZXI	0.018705 -0.003404i	XXIIXXII	0.019597 -0.003566i	IIYYXXY	0.012201 -0.002220i
IIIZIIZI	-0.231557+0.112195i	IIIZIIZ	0.128680 -0.023416i	YZYIXZXI	0.027826 -0.005063i
IYYYYII	0.020481 -0.003727i	IIIXZXZ	0.020604 -0.003749i	IIIXZXI	-0.030067+0.081498i
IYYIYYI	-0.000541+0.000098i	IYYIYZZY	0.006593 -0.001200i	YZYIYZYI	0.027826 -0.005063i
IIIZIXXI	0.033580 -0.006110i	IIXXYZZY	-0.031698+0.005768i	IIIIIZI	-0.611815+0.267480i
IIIIIZZ	0.107859 -0.019627i	YZZYIXXI	0.004990 -0.000908i	IIIIIXZ	-0.012982+0.018373i

TABLE VI: The coefficients and tensor product operators in H_2^- 's complex-rotated Hamiltonian at $\theta = 0.18$, $\alpha = 1.00$ when using 6-31g basis set.

COMPLEX-SCALED HAMILTONIAN OF H_2^- AT $\theta = 0.18$, $\alpha = 1.00$

(Continued)

IXXIXXII	0.003919 -0.000713i	IIZIIII	-0.612966+0.271036i	XZXIIFYZY	0.017127 -0.003117i
IIXXIXXI	-0.000541+0.000098i	IIIIYYII	0.000598 -0.021276i	YYIIHXX	0.021209 -0.003859i
XZZXYIYI	-0.016647+0.003029i	XZXZIIII	0.020644 -0.003757i	YZZYIIYY	-0.029557+0.005379i
YYXXIIII	0.002957 -0.000538i	YZYIIIZI	0.032587 -0.005930i	IIXXYIYI	0.020481 -0.003727i
IXZXIXZX	0.015728 -0.002862i	IXZXIIZI	0.026040 -0.004739i	XYYXIIII	0.012162 -0.002213i
ZIHXZXI	0.038659 -0.007035i	IIXXIIYY	0.034554 -0.006288i	YYIIHYY	0.021209 -0.003859i
IZZIIII	0.087497 -0.015922i	IZIHZII	0.094105 -0.017124i	IYYXXII	0.020481 -0.003727i
IIIZIYZY	0.038191 -0.006950i	IYYIIHXX	-0.002794+0.000508i	IXXIXZZX	0.006593 -0.001200i
IIIZXZX	0.013729 -0.002498i	IIIIYYI	-0.007550+0.006494i	IIIZIZI	0.103932 -0.018913i
YYIIXZZX	-0.019254+0.003504i	IXXIIII	-0.009705+0.008779i	IIHXXII	0.000598 -0.021276i
XZZXIYYI	0.004990 -0.000908i	IZIIHIZ	0.110454 -0.020099i	IZIIIII	-0.388873+0.102313i
IYZYIZII	0.012371 -0.002251i	IXXIIYYI	0.008283 -0.001507i	IYYIYYII	0.003919 -0.000713i
YYIIHXXI	0.005216 -0.000949i	XXYIHHI	0.002957 -0.000538i	IXXIYYII	0.003919 -0.000713i
IIIIYZYZ	0.020604 -0.003749i	IIIIYZYI	-0.030067+0.081498i	IYZYIYZY	0.015728 -0.002862i
IZIHXZXI	0.013080 -0.002380i	IIIIIII	1.734311 -1.110499i	IIIIHIZ	-0.896247+0.369556i
IIZIIZX	0.024717 -0.004498i	IZIHXZX	0.013159 -0.002395i	IIIZIIZI	0.120598 -0.021945i
XZZXIIYY	-0.029557+0.005379i	IIHXYYX	0.012201 -0.002220i	IYZYZIII	0.034152 -0.006215i
IYYIIIII	0.047746 -0.040370i	IXZXYZYI	0.018705 -0.003404i	XZXIIHIZ	0.052229 -0.009504i
XZXIIIII	-0.021561+0.077956i	XZZXXXII	-0.016647+0.003029i	ZIIIIYZY	0.030922 -0.005627i
YIYIIIII	0.017118 -0.003115i	IYYIXZZX	0.006593 -0.001200i	XZZXIIII	-0.027204+0.031862i
IIIIYZY	-0.012982+0.018373i	XXIIXZZX	-0.019254+0.003504i	XZXIIZII	0.011702 -0.002129i
ZIIZIIZI	0.102700 -0.018688i	IIHIZIZ	0.092214 -0.016780i	IIHIZII	-0.386698+0.100135i
IYYIIXXI	0.008283 -0.001507i	IIIZIZI	0.105681 -0.019231i	XXIIIII	0.001646 -0.022572i
IIIIYYXX	0.002918 -0.000531i	IZIZIIII	0.092214 -0.016780i	YZYIZIII	0.040337 -0.007340i
XXXXIIII	0.015119 -0.002751i	XZZXIIXX	-0.029557+0.005379i	IIIZIIZI	0.184425 -0.033560i
IIIZIIII	-0.894071+0.367379i	IIZIIZI	0.144136 -0.026228i	IYZYIYZYI	0.018705 -0.003404i

TABLE V: The coefficients and tensor product operators in H_2^- 's complex-rotated Hamiltonian at $\theta = 0.18$, $\alpha = 1.00$ when using 6-31g basis set.

APPENDIX C

How to get complex eigenvalue by the Direct Measurement Method

If the output state Eq. (17) is measured many times, the possibility of obtaining $|0\rangle_a$ state, p , is related to E by the equation

$$p = \frac{E^2}{A^2}, \quad (25)$$

which reveals $|E| = \sqrt{p}A$. To obtain the phase, one way is that we apply a similar circuit for $H'_\theta = xI^{\otimes n} + H_\theta$, where x is a selected real number. Then the updated U'_r leads us to

$$p' = \frac{|x + Ee^{i\varphi}|^2}{A'^2} \quad (26)$$

By applying $|E| = \sqrt{p}A$ to Eq. (26), we can solve the phase φ and finally the complex eigenvalue as

$$Ee^{i\varphi} = \sqrt{p}Ae^{i \cos^{-1} \frac{p'A'^2 - x^2 - pA^2}{2xA\sqrt{p}}} \text{ or } \sqrt{p}Ae^{-i \cos^{-1} \frac{p'A'^2 - x^2 - pA^2}{2xA\sqrt{p}}}. \quad (27)$$

If we expand the exponential term in Eq. (27), it becomes

$$Ee^{i\varphi} = \frac{p'A'^2 - x^2 - pA^2}{2x} + i \frac{\sqrt{(2xA\sqrt{p})^2 - (p'A'^2 - x^2 - pA^2)^2}}{2x}. \quad (28)$$

Since the measurement errors for p and p' , i.e. $\Delta(p)$ and $\Delta p'$, are $O(\frac{1}{\sqrt{N}})$, based on Eq. (28) the error for the complex eigenvalue $Ee^{i\varphi}$ is

$$\Delta(Ee^{i\varphi}) = O\left(\frac{1}{\sqrt{N}}\right) \quad (29)$$

The larger the sampling size, the more accurate obtained complex eigenvalues are.

There are also other choices to obtain the phase. For example, instead of adding the $I^{\otimes n}$ part, we can try building the U'_r based on $H_\theta + H_\theta^2$ or $H_\theta + H_\theta^3$ to get an equation like Eq.(26) containing phase information. That equation together with Eq.(25) will reveal the complex eigenvalue for the input eigenstate with another expression.

APPENDIX D

A. The Hamiltonian and complex eigenvalue for the model system: n = 2, 5 qubits

The complex-rotated Hamiltonian of the model system is

$$H_\theta = 1.31556 * e^{-0.04180i} II + 0.13333 * e^{2.32888i} YY + 0.13333 * e^{2.32888i} XX + 0.25212 * e^{3.05283i} ZI + 1.06378 * e^{3.11093i} IZ. \quad (30)$$

By running the circuit FIG. 4 for H_θ and a similar circuit for $H'_\theta = xII + H_\theta$, the complex eigenvalue can be derived by

$$Ee^{i\varphi} = \sqrt{p}Ae^{i \cos^{-1} \frac{p'A'^2 - x^2 - pA^2}{2xA\sqrt{p}}} \text{ or } \sqrt{p}Ae^{-i \cos^{-1} \frac{p'A'^2 - x^2 - pA^2}{2xA\sqrt{p}}}, \quad (31)$$

where A and A' can be obtained from the absolute value of coefficients in H_θ and H'_θ , p and p' can be obtained from measurement results.

B. The Hamiltonian and complex eigenvalue for the model system: n = 2, 4 qubits

The complex-rotated Hamiltonian of the model system without II term is

$$H_\theta = 0.13333 * e^{2.32888i} YY + 0.13333 * e^{2.32888i} XX + 0.25212 * e^{3.05283i} ZI + 1.06378 * e^{3.11093i} IZ. \quad (32)$$

If we choose $H'_\theta = H_\theta + H_\theta^3$, which has the same terms of tensor products as H_θ with different coefficients, by running FIG.5 the complex eigenvalue for the original Hamiltonian can be represented by

$$Ee^{i\varphi} = (1.31441 - 0.05497i) + \sqrt{p}Ae^{\frac{i}{2} \cos^{-1} \left(\frac{p'A'^2}{2p^2A^4} - \frac{1}{2pA^2} - \frac{pA^2}{2} \right)} \text{ or} \quad (33)$$

$$(1.31441 - 0.05497i) + \sqrt{p}Ae^{-\frac{i}{2} \cos^{-1} \left(\frac{p'A'^2}{2p^2A^4} - \frac{1}{2pA^2} - \frac{pA^2}{2} \right)}, \quad (34)$$

where A and A' can be obtained from the absolute value of coefficients in H_θ and H'_θ , p and p' can be obtained from measurement results.

C. The Hamiltonian and complex eigenvalue for the model system: n = 2, 3 qubits

The square of the Hamiltonian Eq. (32) is

$$H_\theta^2 = 1.19577 * e^{-0.09723i} II + 0.53529 * e^{-0.05311i} ZZ \quad (35)$$

If we choose $(H'_\theta)^2 = H_\theta^2 + H_\theta^4$, by running FIG.6 the complex eigenvalue for the original Hamiltonian is

$$Ee^{i\varphi} = (1.31441 - 0.05497i) + p^{\frac{1}{4}}\sqrt{A}e^{\frac{i}{2} \cos^{-1} \left(\frac{p'A'^2}{2p^{\frac{3}{2}}A^3} - \frac{1}{2\sqrt{p}A} - \frac{\sqrt{p}A}{2} \right)} \text{ or} \quad (36)$$

$$(1.31441 - 0.05497i) + p^{\frac{1}{4}}\sqrt{A}e^{-\frac{i}{2} \cos^{-1} \left(\frac{p'A'^2}{2p^{\frac{3}{2}}A^3} - \frac{1}{2\sqrt{p}A} - \frac{\sqrt{p}A}{2} \right)} \quad (37)$$

where A and A' can be obtained from the absolute value of coefficients in H_θ^2 and $H_\theta^2 + H_\theta^4$, p and p' can be obtained from their measurement results.

APPENDIX E

QUANTUM CIRCUIT FOR COMPLEX-SCALED HAMILTONIAN OF H_2^- AT $\theta = 0.18$, $\alpha = 1.00$

The complex-scaled Hamiltonian of H_2^- at $\theta = 0.18$, $\alpha = 1.00$ in Appendix B can be written as

$$\begin{aligned}
H = & 0.019012 * e^{-0.180013i} IXZXXZ XI + 0.038818 * e^{-0.180010i} IIIZIXZX + \\
& 0.105638 * e^{-0.180005i} ZIZIIIII + 0.028282 * e^{-0.179983i} XZXIXZ XI + \\
& \dots + 0.019012 * e^{-0.180013i} IYZYYZYI.
\end{aligned} \tag{38}$$

We would like to mention that the terms explicitly shown in Eq. (38) are following the order in Appendix B. It is a coincident that their phases are similar. For example, one term we didn't show in the Hamiltonian is $0.021284 * e^{1.542696i} IIIIYYII$, which has a different phase.

To construct the quantum circuit for Direct Measurement method, we need to create B gate and V gate. The B gate can be prepared by the coefficients from the Hamiltonian Eq. (38)

$$\beta = \begin{matrix} & \begin{matrix} index \\ 0 \\ 1 \\ 2 \\ 3 \\ \vdots \\ 200 \\ 201 \\ 202 \\ \vdots \\ 255 \end{matrix} \\ \begin{matrix} 0.019012 \\ 0.038818 \\ 0.105638 \\ 0.028282 \\ \vdots \\ 0.019012 \\ 0 \\ 0 \\ \vdots \\ 0 \end{matrix} \end{matrix}, \tag{39}$$

as shown in Eq. (15). The V gate can be constructed by a series of controlled- V_i gates, where V_i are

$$V_0 = e^{-0.180013i} IXZXXZ XI, \tag{40}$$

$$V_1 = e^{-0.180010i} IIIZIXZX, \tag{41}$$

$$V_2 = e^{-0.180005i} ZIZIIIII, \tag{42}$$

$$V_3 = e^{-0.179983i} XZXIXZ XI, \tag{43}$$

$$\vdots \tag{44}$$

$$V_{200} = e^{-0.180013i} IYZYYZYI. \tag{45}$$

The whole circuit is shown in the FIG. 8. The encoding of control qubits is based on the binary form of V_i 's index i . For example, V_3 is applied to $|\psi\rangle_s$ if the ancilla qubit state is $|3\rangle_a = |00000011\rangle_a$.

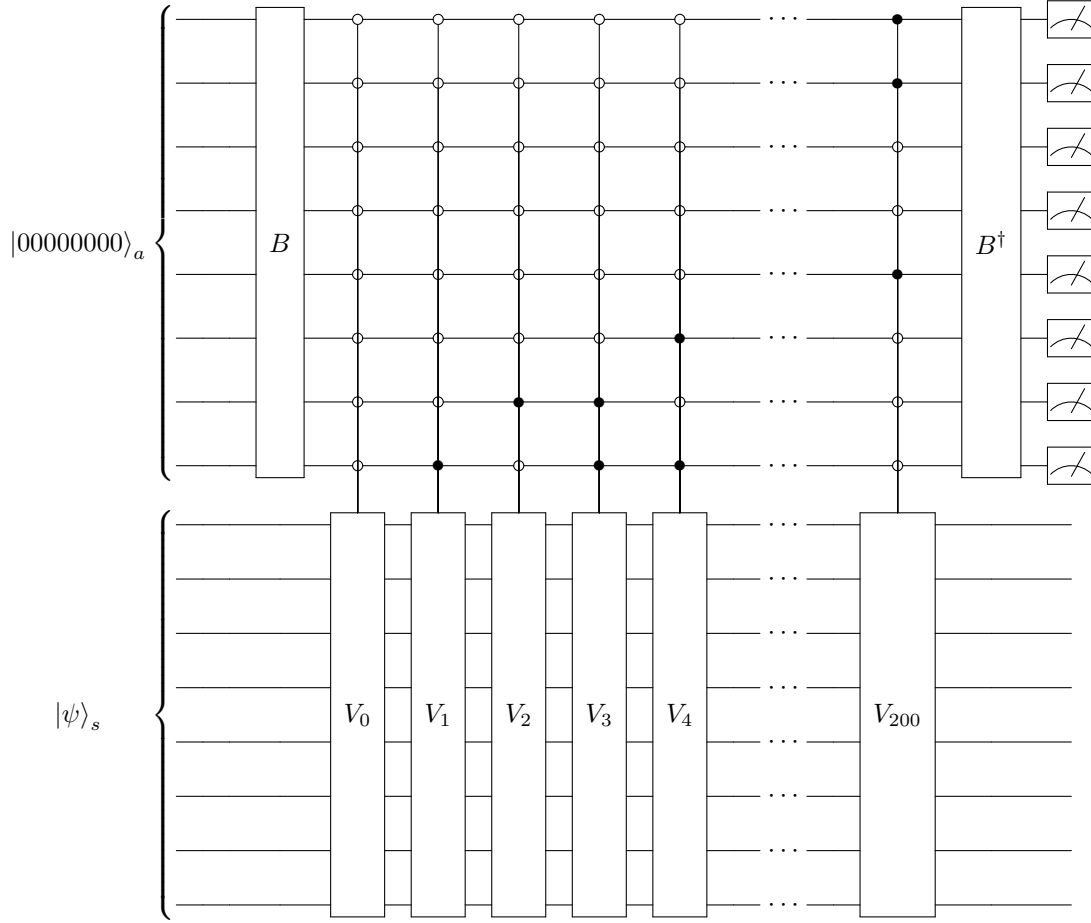


FIG. 8: The quantum circuit to run the Direct Measurement method for H_2^- when $\theta = 0.18, \alpha = 1.00$. B gate can be prepared by β in Eq. (39). V_i gates are listed in Eq. (45).